machines

MDPI

Article

A Study on the Wear Characteristics of a Point Contact Pair of Angular Contact Ball Bearings Under Mixed Lubrication

Yongjian Yu [1,2,3,4], Zifan Dong [1], Yujun Xue [1,2,3,4,*], Haichao Cai [1,3] and Jun Ye [1,4]

[1] School of Mechanical and Electrical Engineering, Henan University of Science and Technology, Luoyang 471003, China; yuyongjian@haust.edu.cn (Y.Y.); 220320010020@stu.haust.edu.cn (Z.D.); chc1226@haust.edu.cn (H.C.); 9905660@haust.edu.cn (J.Y.)
[2] Longmen Laboratory, Luoyang 471000, China
[3] Henan Key Laboratory for Machinery Design and Transmission System, Henan University of Science and Technology, Luoyang 471003, China
[4] Henan Collaborative Innovation Center for High-End Bearings, Luoyang 471003, China
* Correspondence: yjxue@haust.edu.cn

Abstract: Under mixed lubrication, the macro size is affected by the wear of the surface roughness peaks, which results in degradation of the bearing accuracy. To study the wear characteristics of rolling bearings under mixed lubrication, based on the elastohydrodynamic lubrication theory and Archard wear model, and considering the coupling of the oil film and roughness, a wear prediction model of angular contact ball bearings under mixed lubrication was established, and the influence of the working parameters and hardness on bearing wear was analyzed. The results show that the wear depth of the outer grove increases with an increase in the load, or a decrease in the rotational speed or the initial viscosity of lubricating oil. The load has the most significant effect on the wear depth of the outer grove. There is a critical value for the load, rotational speed, and initial viscosity of the lubricating oil, which varies with the parameters of other working conditions and the hardness of the materials. When the increase in load exceeds the critical value or the rotational speed and initial viscosity of lubricating oil are less than the critical value, the outer groove fails because the wear depth exceeds the critical value of wear depth. The ratio of the load on the rolling element to the hardness of the outer grove at different entrainment speeds and initial viscosities of lubricating oil can be used to predict the wear degree of the outer grove. When the ratio is greater than a certain threshold, the outer grove is faulted owing to wear, and the threshold decreases with an increase in the initial viscosity of lubricating oil or the decrease in rotational speed.

Keywords: angular ball bearing; bearing wear; mixture lubrication; surface roughness

check for updates

Academic Editors: Kai Cheng and Candida Petrogalli

Received: 26 February 2025
Revised: 29 March 2025
Accepted: 9 April 2025
Published: 11 April 2025

Citation: Yu, Y.; Dong, Z.; Xue, Y.; Cai, H.; Ye, J. A Study on the Wear Characteristics of a Point Contact Pair of Angular Contact Ball Bearings Under Mixed Lubrication. *Machines* **2025**, *13*, 312. https://doi.org/10.3390/machines13040312

Copyright: © 2025 by the authors. Licensee MDPI, Basel, Switzerland. This article is an open access article distributed under the terms and conditions of the Creative Commons Attribution (CC BY) license (https://creativecommons.org/licenses/by/4.0/).

1. Introduction

Angular contact ball bearings are widely used in high-precision rotating parts due to their high precision, high speed, and ability to withstand axial and radial loads. The types of lubricants used in bearings in different environments are different: when a good sealing environment and medium-speed and low-speed working conditions are required, the bearings are mostly grease-lubricated; under higher working stability and high-speed working conditions, oil lubrication can better transfer heat to maintain better working performance of the bearing; for a working environment with extremely high temperature, high vacuum, strong radiation, and the need to avoid grease pollution, solid lubricants are used to achieve bearing lubrication [1]. Due to factors such as fracture, corrosion,

deformation, and wear, the bearing may fail. The main failure form of the bearing is fatigue wear. However, when the bearing is under harsh lubrication conditions, the bearing surface is in contact with wear, and continuous wear will cause the bearing geometry to change, resulting in a decrease in bearing accuracy and even a loss of accuracy [2–4]. Therefore, it is necessary to study the fluid–solid coupling wear mechanism of angular contact ball bearings.

In the study of the causes of wear on the two surfaces of contact under mixed lubrication, scholars have found that roughness is an important factor affecting lubrication and wear [5–7]. Under the mixed lubrication state, when the lubricating oil film is not separated from the roughness, it causes the roughness to contact and wear [8]. Based on the theory of elastohydrodynamic lubrication and the Archard wear model, scholars have extensively studied the lubrication and wear characteristics of point contact and line contact pairs under mixed lubrication.

In the study of point contact wear under mixed lubrication, aiming to explore the distribution of oil film and pressure in the contact zone under mixed lubrication, Zhu et al. [9–11] proposed a calculation model of point contact wear under mixed lubrication based on the Archard wear model. The model can predict the micro surface wear with time. Considering the wear flash temperature, Pei [12] established a calculation model for point contact wear under mixed lubrication and studied the wear characteristics of point contact pairs. The results show that the load and slide–roll ratio significantly increase the material wear rate, and the friction coefficient decreased rapidly and then tended to stabilize with the occurrence of wear. Considering the influence of roughness, Zhao et al. [13] established a point contact wear calculation model under mixed lubrication considering the influence of roughness and analyzed the influence of surface roughness peak skewness and kurtosis on the wear characteristics and mixed lubrication performance. The results show that increasing the surface skewness and kurtosis will increase the probability of wear, resulting in increased cumulative wear, friction coefficient, and maximum flash temperature rise. Considering the influence of any direction of rolling and sliding speed and surface morphology, Pu and Wang et al. [14,15] established a mixed lubrication calculation model of elliptical point contact pairs. The results show that surfaces with longitudinal roughness texture and a high wavelength ratio are more conducive to improving lubrication performance and reducing wear. Considering the surface roughness and the non-Newtonian characteristics of lubricating oil, Liu et al. [16] established a point contact wear model under mixed lubrication, used the ball-disk wear test to verify the model, and analyzed the influence of lubricating oil film parameters on the wear performance of bearing materials. The results show that the load and speed have a significant effect on the wear coefficient of bearing materials. Scholars' research has focused on the wear and lubrication characteristics of the point contact pair between the ball and plane, but there are relatively few studies on the point contact pair combined with the actual structure of the bearing grove and rolling element.

Aiming at the research of bearing wear, Niu [17,18] analyzed the phenomenon of bearing wear aggravation caused by the change in bearing material properties and lubrication state under a high-temperature environment, established the dynamic wear model of high-temperature angular contact ball bearing, and verified this using experiments. The results show that with the increase in load, speed, and temperature, the wear rate of the inner and outer grove of the bearing increases continuously, and the load and speed are the main factors determining the wear life of the bearing. The stability of the bearing motion is improved to a certain extent with the increase in wear time, but the stability of the bearing motion state deteriorates when the bearing wear is more serious. Chen et al. [19,20] established a hybrid thermal elastohydrodynamic lubrication and wear coupling model for the main bearing of a large low-speed machine under heavy load conditions and analyzed

the wear distribution and evolution of the main bearing during the start-up process. The results show that with the increase in the start-up time, the wear area increases from the center of the bearing area along the circumferential direction of the bearing, the contact pressure decreases, the oil film pressure decreases slightly, and the lubrication performance is improved. Based on the dry friction test, Colas et al. [21] compared the effects of four self-lubricating materials on the wear performance. The results show that high-adhesion materials can easily increase the wear of the bearing surface. Considering the influence of surface roughness, Shi and Feng et al. [22–26] established a mixed lubrication wear model of ball bearings and analyzed the friction and wear characteristics of bearings. The results show that a heavy load and low speed lead to an increase in the dry contact zone and the friction temperature, and the deterioration state become worse, which may further cause the failures of mass wear, scuffing, and micro pitting.

In summary, the current research focuses on the changing trends in the friction coefficient, oil film, pressure, contact roughness characteristics, and other parameters of the bearing contact pair. However, during the bearing working process, the wear depth of the bearing accumulates continuously, which ultimately affects the macroscopic size parameters of the bearing and causes the bearing accuracy to decline. Therefore, the wear depth of the bearing is related to its accuracy, and there are relatively few studies on the change in the wear depth of the bearing. Therefore, based on the theory of elastohydrodynamic lubrication and Archard wear theory, and considering the coupling relationship between the lubricating oil film and the roughness and the influence of fluid–solid coupling, a wear prediction model of an angular contact ball bearing under mixed lubrication is established. The analysis of the change in bearing wear depth under mixed lubrication is helpful for further deepening the understanding of the change law of bearing wear under mixed lubrication, reducing the wear of the bearing surface, and improving the accuracy retention of the bearing.

2. Wear Prediction Model of Angular Contact Ball Bearing Under Mixed Lubrication Condition

Based on the mixed lubrication wear theory, the oil film thickness equation considering the coupling of surface roughness and lubricating oil is combined with the pressure equation and viscous pressure equation, which jointly constructs the Reynolds equation under the coupling of asperity and flow field. Based on the Reynolds equation, and combined with the motion parameters of the bearing grove and the rolling element calculated by the pseudo-dynamic model, the pressure of the contact zone between the bearing grove and the rolling element and the contact condition of the roughness under mixed lubrication are found. Combined with the Reynolds equation and the modified Archard wear model to solve the contact zone parameters, the bearing wear in the contact zone is calculated. After calculating the wear height of the roughness in the contact area, the wear height is subtracted from the corresponding position of the original roughness to obtain the relative roughness of the two contact surfaces after wear. If the calculation step is not set, the two surface roughness values are translated at different distances to achieve the phenomenon of two surface movements, which makes the model fitting more realistic. The moving wear roughness is brought into the Reynolds equation to calculate the next long wear until the preset number of steps is reached. The basic process is illustrated in Figure 1.

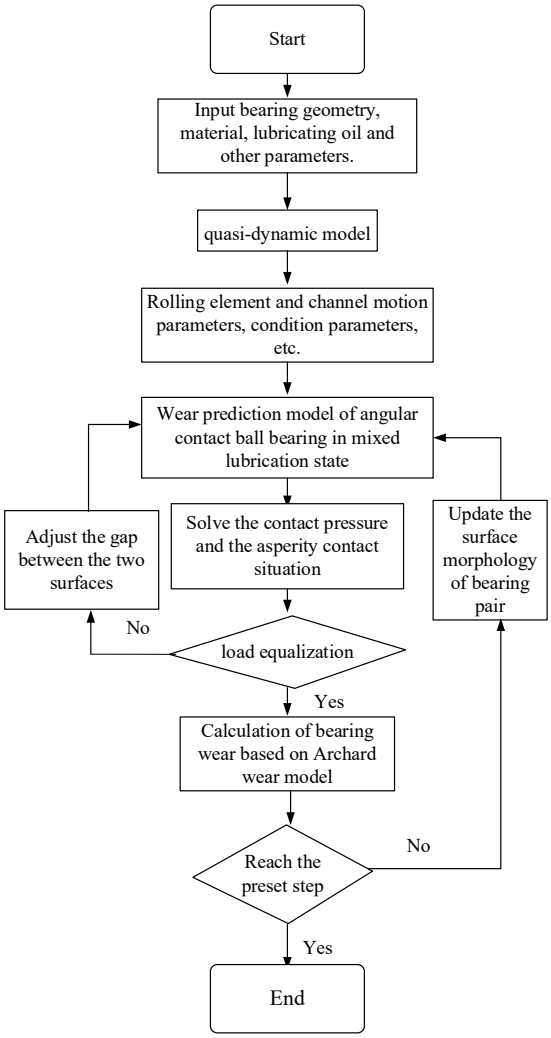


Figure 1. Model calculation process.

2.1. Solving the Basic Equation of Mixed Lubrication

In this study, in the mixed lubrication state, the contact area is divided into the fluid lubrication area Ω_l and the roughness contact area Ω_c. The hydrodynamic pressure p_l in the fluid lubrication area is solved by the Reynolds equation, which is expressed as follows:

$$\frac{\partial}{\partial x}\left(\frac{\rho h^3}{\eta}\frac{\partial p_l}{\partial x}\right)+\frac{\partial}{\partial y}\left(\frac{\rho h^3}{\eta}\frac{\partial p_l}{\partial y}\right)=12\left(u_s\frac{\partial \rho h^3}{\partial x}+\frac{\partial \rho h^3}{\partial t}\right) \tag{1}$$

For the solution of the contact pressure of the roughness in the contact area of the roughness, as there is no oil film at the contact node and the pressure term at the left end is zero, the lubricating oil contact pressure p_l solved by the Reynolds equation is equal to the contact pressure of the roughness p_c, and the Reynolds equation after closing the pressure term is as follows:

$$u_s\frac{\partial h}{\partial x}+\frac{\partial h}{\partial t}=0 \tag{2}$$

When the dimensionless film thickness is less than 1×10^{-7}, the roughness is considered to be contacted, and the dimensionless film thickness of the contact node is set to 1×10^{-7} so that the Reynolds equation solution matrix is diagonally dominant.

The roughness is considered in the film thickness equation and is used as an additional term in the film thickness equation to realize the coupling of roughness and lubrication.

The film thickness equation is as follows (see the symbol table for the parameters in the equation, where h_0 is the initial value of Dowson minimum film thickness [27]):

$$h(x,y,t) = h_0 + \frac{x^2}{R_x} + \frac{y^2}{R_y} + v(x,y,t) + \delta_1(x,y,t) + \delta_{2(x,y,t)} + w_1(x,y,t) + w_2(x,y,t) \quad (3)$$

The solution of the surface elastic deformation of each coordinate point is not only affected by the pressure of the node but also affected by the pressure of adjacent nodes. Therefore, the calculation of the surface elastic deformation of each coordinate point adopts the numerical integration method, and the specific calculation formula is as follows.

$$v(x,y,t) = \frac{2}{\pi E}\iint_{\Omega} \frac{p_l(s,r,t) + p_c(s,r,t)}{\sqrt{(x-s)^2 + (y-r)^2}} \quad (4)$$

where s and r are the distance between the solution node and the adjacent node in the x and y directions. The surface elastic deformation of each coordinate point is solved by DC-FFT. The specific solution process can be seen in Reference [7].

The viscosity and density of the lubricating oil are pressure functions, which are calculated using the density pressure equation [28] and the viscosity pressure equation [29].

$$\rho = \rho_0\left(1 + \frac{0.6 * 10^{-9} \times p_l}{1 + 10.7 \times 10^{-9} \times p_l}\right) \quad (5)$$

$$\eta = \eta_0 exp^{\alpha p_l} \quad (6)$$

The model simulation adopts the isothermal model, and the lubricating oil lubrication adopts the aviation lubricating oil. In the calculation, the flash temperature effect caused by the asperity wear and the influence of the bearing temperature rise on the viscosity of the lubricating oil between the rolling element and the outer grove contact pair are not considered. Therefore, after the working temperature of the bearing is set, the initial dynamic viscosity of the model is determined, and it will only be affected by the contact pressure.

Since the height distribution of asperities on machined surfaces follows a Gaussian (normal) distribution, the surface roughness in the model is simulated using Gaussian-distributed random functions. This methodology generates realistic roughness for both contacting surfaces.

$$\delta(\mathrm{x},\mathrm{y}) = \sigma \times \varepsilon_{i,j}(i = 1,2,\cdots,n; j = 1,2,\cdots,n)$$

where $\varepsilon_{i,j}$ is a normal distribution function with a mean value of 0 and the standard deviation of 1. The surface roughness is simulated by controlling σ. The simulated surface is obtained by averaging the data of different directions measured by experiments.

2.2. Solving Boundary Conditions and Convergence Criteria

When the Reynolds equation is used to solve the pressure in the contact zone between the bearing rolling element and the grove, the boundary conditions of the contact region of the Reynolds equation are solved as follows:

$$\begin{cases} p(x,y_0) = 0\ p(x,y_e) = 0 \\ p(x_0,y) = 0\ p(x_e,y) = 0 \\ p(x,y) = 0\ p(x,y) \le 0 \end{cases} \quad (7)$$

The semi-system composite iteration method is used to solve the Reynolds equation. After the equation is unified and dimensionalized, it is discretized by the finite difference method.

$$A_{i,j}P_{i-1,j} + B_{i,j}P_{i,j} + C_{i,j}P_{i+1,j} = Z_{i,j} \tag{8}$$

where $A_{i,j}$, $B_{i,j}$, $C_{i,j}$, $Z_{i,j}$ are composed of the known quantities of the discretized nodes, and $P_{i-1,j}$, $P_{i,j}$, $P_{i+1,j}$ are the dimensionless pressure of the demand solution. The specific solution in the above formula can be seen in Reference [30].

Extract the coefficients on the left side to construct the solution coefficient matrix, and the matrix is solved by the catch-up method. In the process of solving, it is found that the coefficient matrix of the Reynolds equation diverges easily. To solve the divergence problem, the entrainment velocity coefficient and pressure term coefficient are combined to ensure that the coefficient matrix is diagonally dominant, so that the coefficient matrix is solved stably, and the convergence performance of the Reynolds equation is improved.

The load balance principle is used as the convergence criterion for the pressure solution, that is, the relative error between the load (W_z) on the bearing contact zone and the total integral of the pressure in the contact area reaches 1×10^{-3}, to determine the convergence of the model pressure solution [26]. The load balance equation is as follows:

$$\iint_{\Omega_l} p_l(x,y,t)dxdy + \iint_{\Omega_c} p_c(x,y,t)dxdy = W_z \tag{9}$$

If the pressure solution does not reach the convergence standard, combined with the difference between the total integral of the pressure and the normal load of the contact area, the undeformed gap between the two surfaces of the new rolling element and the contact area of the channel is calculated. The calculation formula is

$$\Delta W = \frac{W_z - \iint_\Omega (p_l(x,y,t) + p_c(x,y,t))dxdydxdy}{Wz} \tag{10}$$

$$h_o = h_0' - \Delta W \times h_{min} \tag{11}$$

The gap adjustment changes the film thickness distribution so that the Reynolds equation is solved to make the contact pressure distribution closer to the convergence value. This solution process is repeated until the end of the pressure solution iteration.

2.3. Wear Calculation of Roughness

The wear height of the asperity in the film thickness equation is calculated according to the wear height calculation method proposed by Meng et al. [31].

$$\mathrm{w} = \frac{V}{At} = K\frac{WL}{AHt} = K\frac{p_c L}{Ht} = K\frac{p_c \Delta u}{H} \tag{12}$$

In order to speed up the calculation speed, the wear coefficient is equivalently amplified based on the Archard wear theory. The relationship of the wear coefficient equivalently amplified by N times is

$$V = K\frac{W \times \Delta u \times t}{H} = K\frac{W \times N \times \Delta u \times \Delta t}{H} = K_1\frac{WL}{H} \tag{13}$$

The magnification of the wear coefficient is too small, and the model simulation time is too long, which affects the calculation efficiency. The wear coefficient magnification is too large, and the calculation speed is improved, but the error of the simulation results is large. Therefore, it is necessary to select the appropriate magnification, combined with the

corresponding time step, to achieve the objective of predicting the wear of angular contact ball bearings under mixed lubrication.

3. Model Validation Experiment

In order to obtain the wear coefficient required by the wear prediction model of mixed lubrication angular contact ball bearing and to verify the rationality of the model, the wear test was carried out by using the ball-on-disk test machine in Figure 2, and the normal load of the contact point was applied by the lever principle. The experimental conditions of different slide–roll ratios are realized by using two servo motors to control the rotation speed of the test ball and the test disk. The surface topography parameters related to the surface roughness peak before wear and the surface topography of the wear area of the disk sample were measured by the surface topography instrument in Figure 3. The test machine measures the surface topography by applying a small normal load to the probe and the up and down displacement of the probe. During measurement, the surface roughness parameters are obtained by measuring the multi-directional rough peak parameters and taking the average value.

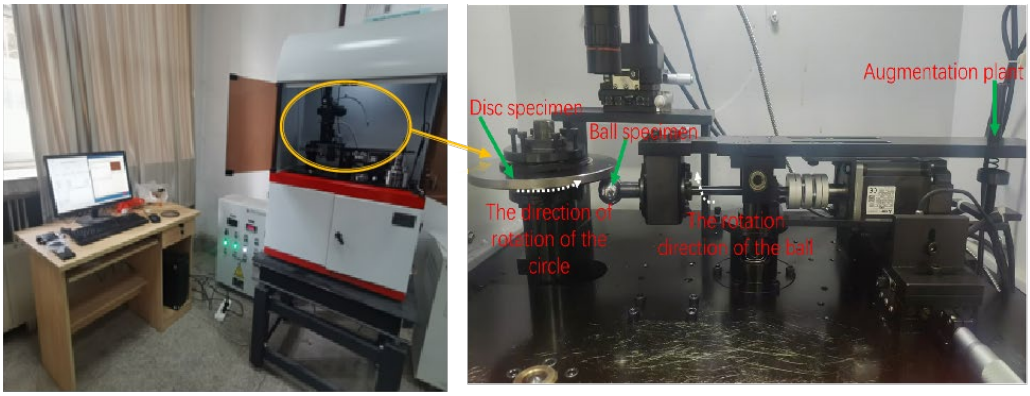


Figure 2. Spherical disk testing machine.

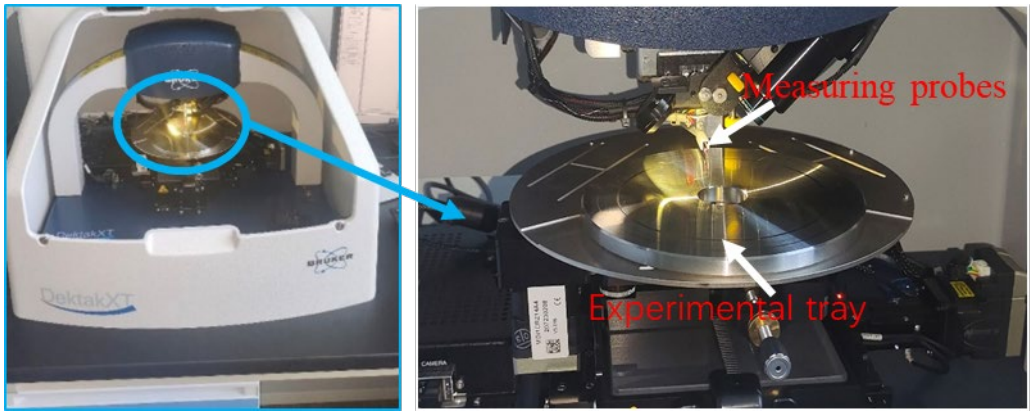


Figure 3. Surface topography measuring instrument.

In the ball-on-disk test, the material of the test piece is GCr15. The diameter of the experimental ball used in the test is 25.4 mm, its surface roughness is 0.016 μm, and its hardness is 64HRC. The test temperature is 30 °C. Table 1 shows the specific material parameters of the steel ball and steel disk.

Table 1. Material parameters of experimental steel ball and experimental steel disk.

	Test Disk	Test Ball
Young's modulus/GPa	208	210
Poisson ratio	0.3	0.3
Density/(g/cm^3)	7.865	7.865

3.1. Rolling–Sliding Composite Dry Friction and Wear Coefficient

Because the dry friction and wear coefficient are used to calculate the rough wear in the model, the rolling–sliding dry friction and wear test is carried out to obtain the rolling–sliding composite dry friction and wear coefficient. The specific working conditions are shown in Table 2 below.

Table 2. Real rolling–sliding dry friction experimental conditions.

Test Conditions	1	2	3	4
Load/N	75	75	75	70
Test disk line speed/(m/s)	0.99	0.63	0.45	0.63
Test ball line speed/(m/s)	0.81	1.17	1.35	1.17
Test disk hardness/HRC	26	26	26	45
Test disk wear radius (d)/mm	54	59	64	52
Test temperature/°C	30	30	30	30
Test disk surface roughness Ra/μm	0.0513	0.0513	0.0513	0.0762
Experimental ball surface roughness Ra/μm	0.0199	0.0199	0.0199	0.0199
Wear time/h	4	4	2.5	4

The wear coefficient of the material is calculated using the Archard wear model. The solution principle can be seen in Reference [32]. The calculation diagram of wear coefficient is shown in Figure 4.

$$K = \frac{VH}{WL} = \frac{A_1 \times D \times H}{W \times \Delta U \times t} \tag{14}$$

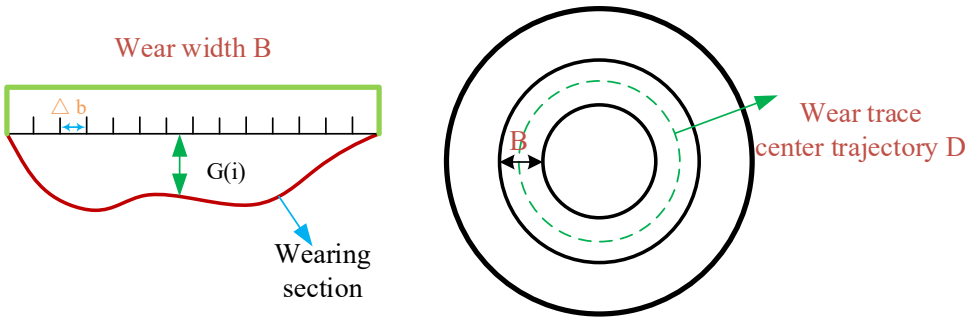


Figure 4. Wear trace parameters.

In Equation (14), A_1 divides the wear width B into I equal parts according to the measurement interval Δb of the surface topography measuring instrument, and each measurement point corresponds to a wear height $G(i)$. The equal interval is multiplied by the corresponding wear height of each measurement point and then added together to obtain the following:

$$A_1 = \sum_{z=1}^{i} G(i) \times \Delta b \tag{15}$$

After measurement and calculation, the average wear coefficient of the 26 HRC experimental disk is about 1.25×10^{-4}; the average wear coefficient of the 45 HRC disk is

2.48×10^{-5}. The following figure is the mean and standard deviation of the wear coefficient of each experimental group. The experimental results of each group are shown in Figure 5.

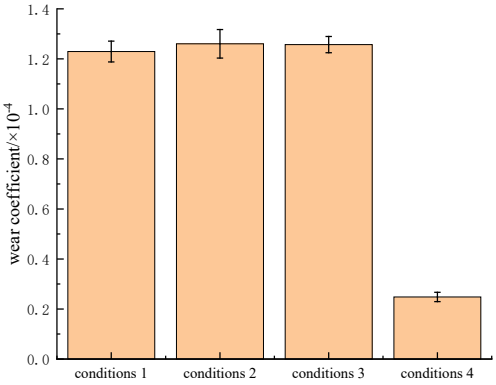


Figure 5. The average value and standard deviation of the wear coefficient of each group in the dry friction and wear test.

3.2. Mixed Lubrication Test Verification

To determine the rationality of the model, the ball-disk tester shown in Figure 3 was used to perform the wear experiment under mixed lubrication, and the model simulation results were compared with the experimental data to verify the rationality of the model.

The ratio of the minimum film thickness of DOWSON to the root mean square (RMS) of the composite roughness from both contacting surfaces was calculated. The formula for calculating the film thickness ratio is

$$\lambda = \frac{h_{min}}{\sigma_0} \tag{16}$$

In this study, the initial film thickness ratio is defined as the ratio of the minimum film thickness to the root mean square of surface roughness peaks on unworn surfaces; it can reflect the lubrication state of the rolling element and the outer grove and judge whether the bearing contact pair is in a non-full film lubrication state. Ensure that the test condition is in a mixed lubrication condition. For post-wear conditions, the film thickness ratio calculation requires re-evaluating the equivalent composite roughness (the composite RMS roughness from both contacting surfaces) and substituting this updated value into the formula.

The test conditions are as follows: the entrainment speed is 0.5 m/s, and the slide–roll ratio is S = 1.0, and the normal load is 75 N. The hardness of the disk specimen in the model is 26HRC, the test disk surface roughness Ra is 0.0513 μm, and the experimental ball surface roughness Ra is 0.0199 μm. Combined with amplification formula (13) and the related literature [12], the equivalent wear coefficient of the simulation is 0.0004 for the steel ball and 0.03 for the disk. The mesh density of the model contact zone is 65×65, the mesh size is 0.023 mm, the viscosity of the lubricating oil is 0.058 Pa·s, and the initial film thickness ratio is 1.105.

The simulation results used the wear prediction model combined with the test verification conditions and were compared with the test results. To improve the calculation accuracy, this study is extracted multiple wear depth curves in the contact zone and calculated the average wear depth curve. The calculation diagram is shown in Figure 6, and it is compared with the experimental measurement parameters.

Figure 7 shows the comparison of the wear cross-section between the test and model simulation. It can be seen from the diagram that the maximum wear depth of the experiment is 3.59 μm, the maximum wear depth of the simulation is 3.44 μm, and the relative error

is 4.3%. The experimental wear width is 0.67 mm, the simulated wear width is 0.62 μm, and the relative error is 8.1%. Therefore, in the micro-morphology of the disk in Figure 8, it can be seen that there are obvious wear marks; the simulated wear cross-section and the experimental wear cross-section show a 'V' shape, and the maximum wear depth position is biased towards the wear center. Because the model only considered the sliding wear factor, there is a certain error in the model calculation. Combined with the verification of experimental data, the model predicts that the wear error is within the reasonable range; therefore, it is feasible to use the model to predict wear.

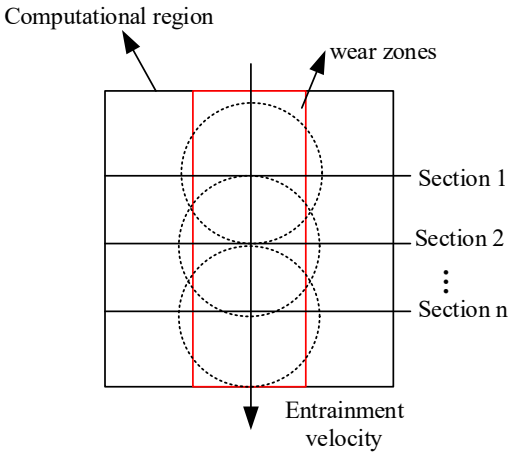
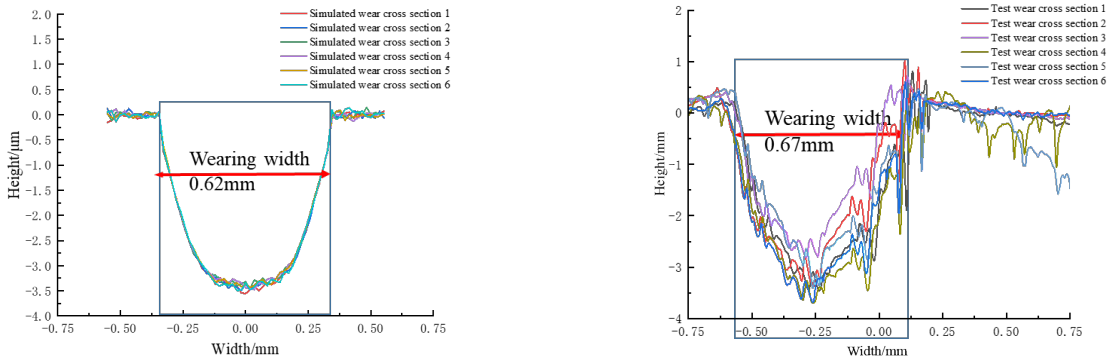
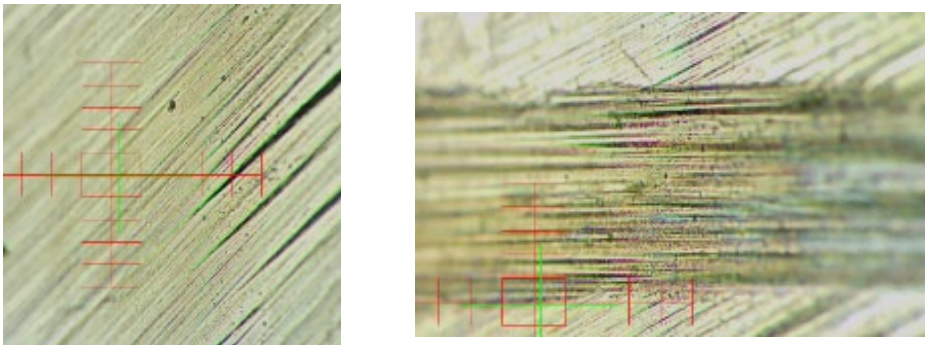


Figure 6. Schematic diagram of model parameter extraction.



(**a**) (**b**)

Figure 7. Comparison of wear cross-sections: (**a**) simulation result; (**b**) test result.



(**a**) (**b**)

Figure 8. The microstructure of the disk specimen under mixed lubrication experimental conditions: (**a**) unworn surface; (**b**) worn surface.

4. Results

Therefore, the 7010 C angular contact ball bearing is taken as the research object, the slide–roll ratio is S = 0.6, and the hardness of grove is 64 HRC. According to the literature [12], the equivalent wear coefficient is 0.005 for the outer grove and 0.002 for the rolling element. The specific parameters of the bearing are shown in Table 3. The relevant parameters of the lubricating oil are shown in Table 3.

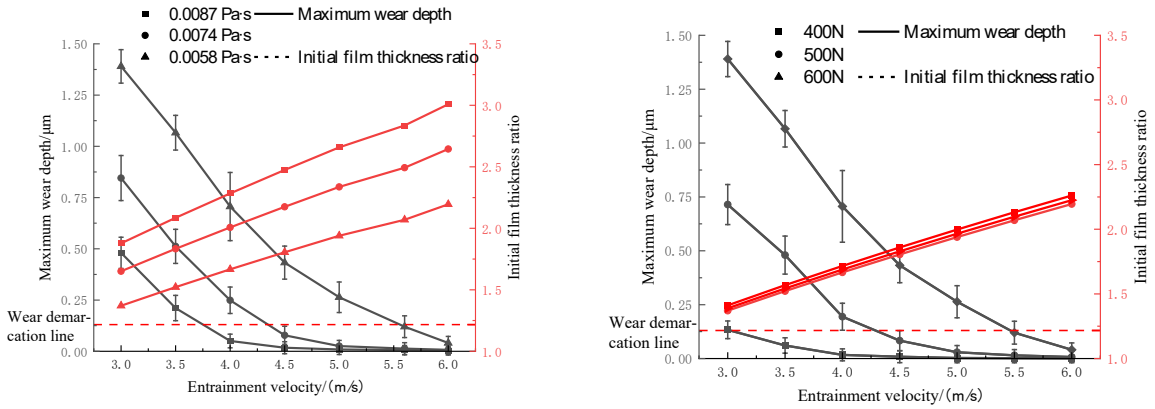
Table 3. Angular contact ball bearing parameters.

Parameter Name	Numerical Value
Material	GCR15
Effective radius in x direction/m	0.00416
Effective radius in y direction/m	0.0506
Outer grove surface roughness/μm	0.0398
Surface roughness of rolling element/μm	0.0199
Elastic modulus of outer grove/GPa	208
Elastic modulus of rolling element/GPa	210
Rolling element and outer grove Poisson's ratio	0.3
Material density of rolling element and outer grove/(kg/m^3)	7830
(40 °C) Dynamic viscosity of lubricating oil/(Pa·s)	0.03947
Lubricating oil density/(g/cm^3)	0.846
Rolling element hardness	64HRC

In the model analysis, the influence of the working condition parameters and material parameters on the outer grove wear of the bearing is analyzed by using the film thickness ratio and the maximum wear depth of the outer grove wear section.

4.1. The Effect of Entrainment Velocity on the Wear of Angular Contact Ball Bearings

Figure 9 shows the relationship between the entrainment speed and the maximum wear depth of the outer grove under different initial viscosities of lubricating oil and the load of the rolling element. It can be observed from the figure that the maximum wear depth of the outer grove decreases with the increase in the entrainment speed. The lower the initial viscosity of the lubricating oil or the greater the load of the rolling element, the more the downward trend in the wear depth has a significant effect.



(**a**) (**b**)

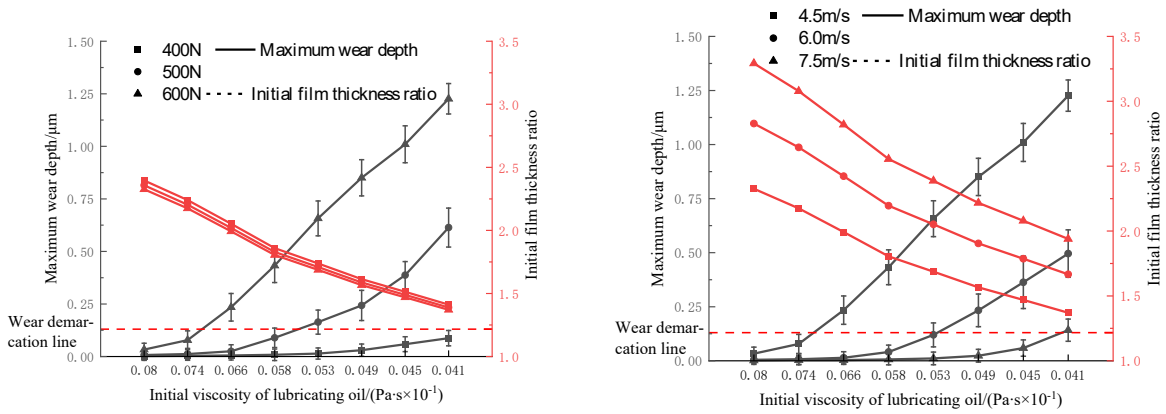
Figure 9. The relationship between entrainment velocity and maximum wear depth: (**a**) 64HRC 600 N different initial viscosity of the lubricating oil; (**b**) 64HRC 0.0058 Pa·s different rolling elements bear the load.

In the process of changing the maximum wear depth of the outer grove of the bearing, there is a specific critical value of the entrainment velocity. When the actual entrainment velocity reaches the critical value, the maximum wear depth of the outer grove is close to 2.8 times the surface root mean square value. Combined with the research on the wear characteristics of engineering materials in the International Business Machines (IBM) laboratory mentioned in Reference [33], it can be seen that when the wear depth does not exceed 2.8 times the surface root mean square value, the wear trace is difficult to observe and the surface damage is small. Once the threshold is exceeded, the wear will significantly increase and seriously affect the performance of the parts. Therefore, we define the wear standard as 2.8 times of the root mean square value of the surface. Therefore, when the running speed of the bearing in the figure is higher than the critical entrainment speed, the wear degree of the outer grove maintains a low level. On the contrary, if the running speed is lower than the critical value, the wear amount will rise sharply.

With a decrease in the initial viscosity of lubricating oil or an increase in the load of rolling element, the critical value of the entrainment velocity increases continuously. This is due to the decrease in the initial viscosity of the lubricating oil or the increase in the load, the decrease in the film thickness ratio, the increase in the rough contact, and the aggravation of the wear, while the increase in the entrainment speed leads to an increase in the film thickness ratio and a decrease in the outer grove wear. This interaction increases the critical value of entrainment velocity. Comparing the influence of the rolling element load and the initial viscosity of the lubricating oil bearing on the critical value of the entrainment velocity, it is found that the influence of the load on the critical value of the entrainment velocity is greater than that of the initial viscosity of the lubricating oil.

4.2. The Effect of Initial Viscosity of Lubricating Oil on Wear of Angular Contact Ball Bearings

Figure 10 shows the influence of the initial viscosity of the lubricating oil on the maximum wear depth of the outer grove under different loads and entrainment speeds. From the diagram, it can be observed that with the decrease in the initial viscosity of the lubricating oil, the wear of the outer grove increases. The load of the rolling element increases or the entrainment speed decreases, and the maximum wear depth of the outer grove increases. However, under low-load conditions, the maximum wear depth of the outer grove does not change significantly with the initial viscosity of the lubricating oil. This is due to the decrease in the load-to-hardness ratio under smaller load conditions. The roughness pressure in the contact zone of the bearing was small, and only the small part of plastic deformation occurred.



(**a**) (**b**)

Figure 10. The relationship between initial viscosity of the lubricating oil and maximum wear depth: (**a**) 64HRC 4.5 m/s different rolling elements bear the load; (**b**) 64HRC 600 N different entrainment speeds.

Comparing Figure 10a,b, it can be seen that when the initial viscosity of the lubricating oil is lower than the critical initial viscosity of the lubricating oil, the wear of the bearing is aggravated. Inversely, the wear of the outer grove is not obvious. The critical value of the initial viscosity of the lubricating oil decreases with the increase in the entrainment speed or the decrease in the load on the rolling element, and the change in the load on the rolling element makes the critical value of the initial viscosity of the lubricating oil corresponding to the wear critical value increase more. Therefore, the influence of the rolling load on the wear of the outer grove is greater than that of the entrainment speed.

4.3. The Effect of Load on the Wear of Angular Contact Ball Bearing

Figure 11 shows the effect of load on the maximum wear depth of the outer grove under different entrainment speeds and initial viscosities of the lubricating oil. From the diagram, it can be observed that as the load of the rolling element increases, the bearing wear of the outer grove increases. When the load of the rolling element is equal to a critical value, the wear depth is equal to the wear depth critical value. When the load exceeded the critical value, the wear of the outer grove increased significantly; inversely, the degree of wear of the outer grove is low. Comparing the different working conditions, it is found that the value increased with the increase in the entrainment speed or the initial viscosity of the lubricating oil. This is due to the low entrainment speed or high viscosity of the lubricating oil conditions; the bearing film thickness is relatively low, the roughness contact was greater, and contact plastic deformation occurred easily.

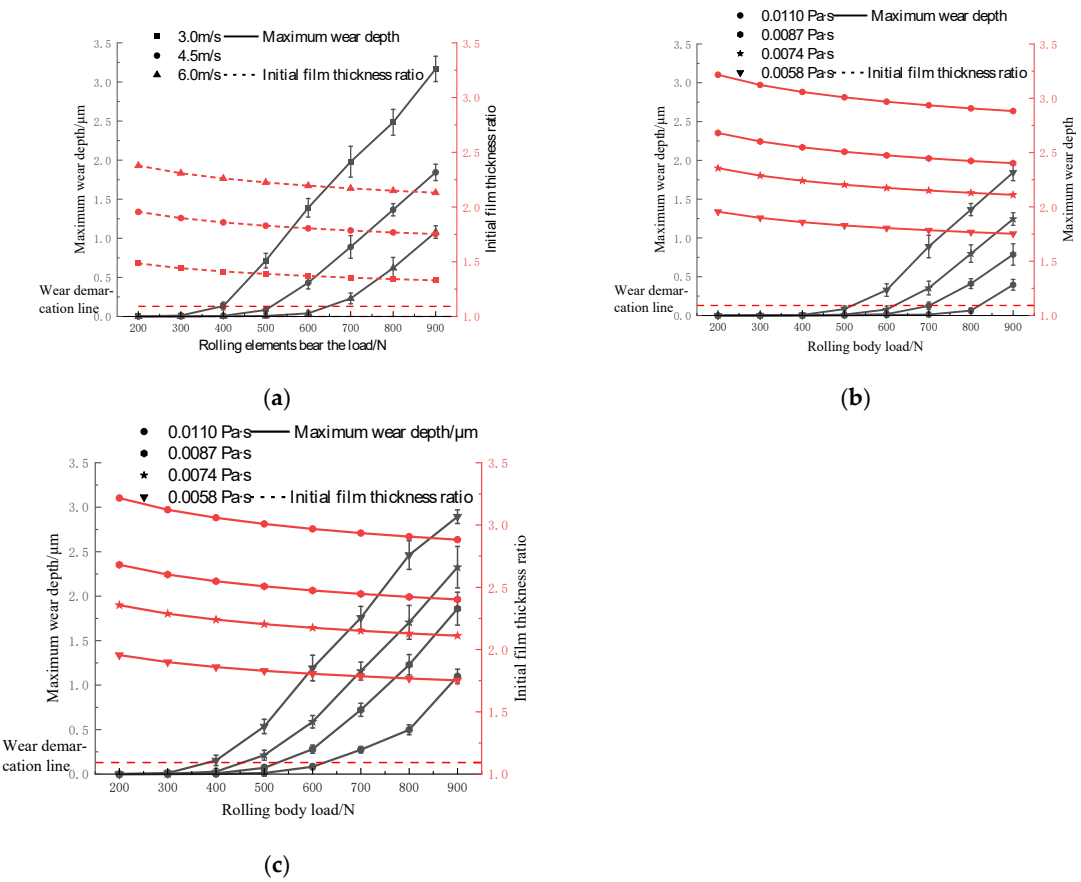


Figure 11. The relationship between the load on the rolling element and the maximum wear depth: (**a**) 64HRC 0.0058 Pa·s different entrainment speeds; (**b**) 64HRC 4.5 m/s different initial viscosity of the lubricating oil; (**c**) 45HRC 4.5 m/s different initial viscosity of the lubricating oil.

Comparing the ratio between the critical load of the rolling element and the hardness of the material under different working conditions in the mixed lubrication state, it is found that the ratio shows a downward trend with the decrease in the bearing initial viscosity of the lubricating oil or the entrainment speed. Combined with the bearing hardness factor, it is found that as the hardness of the bearing material decreased, the ratio increased. However, compared to the ratio change caused by the change in working conditions, the ratio fluctuated less with the change in hardness. This is because the hardness of the material decreased, the yield strength decreased, and the wear increased. It is necessary to reduce the load level of the rolling element to reduce the maximum wear depth, and the proportion of the reduction in the critical load of the rolling element is not equal to the hardness.

4.4. Effect of Hardness of Outer Grove Material on Wear of Angular Contact Ball Bearing

In this section, the influence of the hardness of the grove material on the bearing wear is analyzed. Three hardness values, 64 HRC, 45 HRC, and 26 HRC, were selected. The hardness of the rolling element material is 64 HRC, the entrainment speed is 6.0 m/s, the slide-roll ratio S = 0.6, and the bearing operating temperature is 110 °C. The initial viscosity of the lubricating oil is 0.0058 Pa·s. Owing to the different hardness values of the grove material, the real wear coefficients were also different. Using the Archard wear theory, the grove wear coefficient is uniformly equivalent to 0.005, and the rolling element wear coefficient is equivalent to the grove wear coefficient according to the grove wear coefficient magnification. Table 4 shows the amplification and rolling element wear coefficients.

Table 4. Equivalent enlarged wear coefficient of rolling element with different hardness values.

Hardness	64HRC	45HRC	26HRC
Coefficient of wear	0.002	0.0002	0.00004

Figure 12 shows the relationship between the load of the rolling element and the maximum wear depth of the outer grove under different hardness values. As shown in the figure, as the hardness decreased, the maximum wear depth of the outer grove increased. Under different hardness conditions, the maximum wear depth of the outer grove exceeded that of the wear boundary. With the deterioration of the lubrication state, the trend in bearing wear is obvious. With the decrease in hardness, the critical load value decreases, which is due to the relatively serious wear of low-hardness materials. Reducing the load can increase the film thickness ratio and reduce wear, and the interaction between the two reduces the load of the rolling element value.

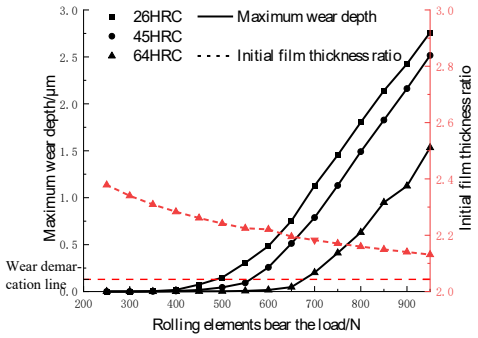


Figure 12. The change in maximum wear depth under different hardness levels.

Figure 13 shows the changing trend in the film thickness ratio to the maximum wear depth with time under different hardness conditions. From the diagram, it can be seen

that under different hardness levels, the changing trend in the film thickness ratio with the time step is consistent, but under different load conditions, the changing trend in the film thickness ratio with the time step is different. When the bearing load is small, after the wear of the higher roughness, the contact pressure of the roughness cannot reach the yield strength, no plastic deformation occurs, and no wear occurs; thus, the film thickness ratio first increases and then tends to be stable. When the bearing was under large load conditions, the film thickness ratio first increased and then decreased. The rate of decrease in the film thickness ratio becomes gentle with the increase in the time step. This is due to the fact that the wear exceeds a certain level of the surface, and the wear of the roughness in the contact zone is reduced. The root mean square growth rate of the surface slows down, which slows down the change in the film thickness ratio. When the load causes the asperity contact pressure in the contact zone to fall between the yield limits of two different hardness, such as the 600 N load of the rolling element condition in the figure, the 64 HRC in the figure has shows less plastic deformation of the asperity in the stable wear stage because of the higher yield strength, and the wear is relatively small. Therefore, the wear depth of the outer grove and the change in the film thickness ratio is relatively small, but the overall trend first increases and then declines steadily. Under the low-hardness condition, the yield strength of the outer grove is low, which makes the outer grove wear more seriously, and the change in the film thickness ratio of the outer grove is similar to that under the high-load condition.

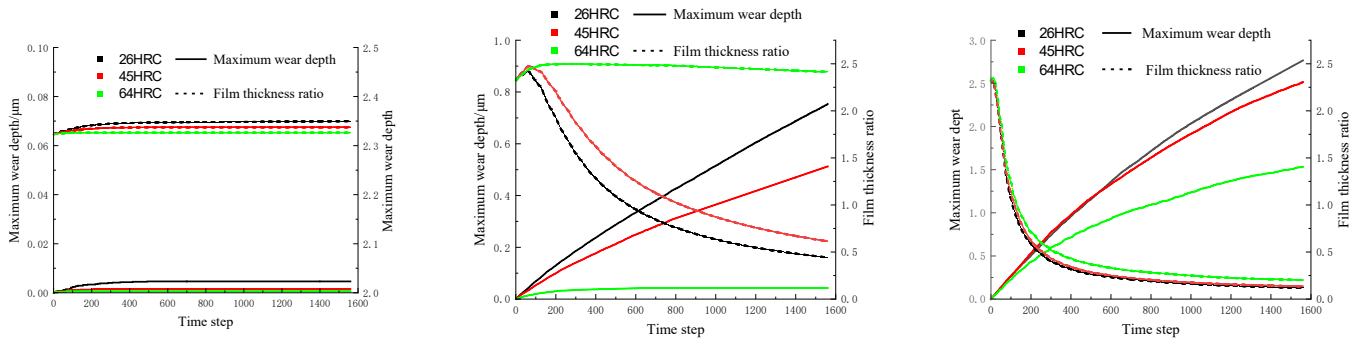


Figure 13. The film thickness ratio of different hardness levels to the maximum wear depth varies with time: (**a**) 300 N; (**b**) 600 N; (**c**) 900 N.

5. Conclusions

In this study, the angular contact ball bearing was considered as the object, and the parameters of the contact area were calculated using the quasi-dynamic model. Combined with the wear prediction model of the angular contact ball bearing under mixed lubrication, the micro surface wear was calculated, and the rationality of the model was verified experimentally. The wear characteristics of the outer grove surface of the bearing under mixed lubrication conditions were analyzed. The following conclusions are drawn:

(1) Under the condition of mixed lubrication, the wear depth of the outer grove increases with the increase in the load of the rolling element, the decrease in the initial viscosity of the lubricating oil, the decrease in the hardness of the raceway material, and the decrease in the bearing speed. The load of the rolling element has the most significant effect on the wear depth of the outer grove. In the mixed lubrication state, by adjusting the matching between the bearing working conditions and the bearing model, the bearing lubrication state is controlled within a certain range, which can effectively reduce wear and improve the bearing precision life.

(2) There are critical values for load, the initial lubricating oil viscosity, and speed, which changes with the change in other working condition parameters. When the initial viscosity of the lubricating oil and load exceed a specific critical value or when the speed is lower than the critical speed, the outer grove wear is significant. The threshold can be used to predict whether the bearing has a wear risk.

(3) The ratio of the load on the rolling element to the hardness of the outer grove of the bearing under mixed lubrication can reflect the wear degree of the outer grove. When the ratio is greater than a certain threshold, the lubrication state of the outer grove will deteriorate. The outer grove will be damaged because the wear depth is greater than the critical value of wear, and the threshold will decrease with the decrease in initial viscosity of the lubricating oil or speed. Combined with the range of bearing operating conditions, the selection of appropriate bearing materials is helpful in reducing bearing wear damage and improving bearing accuracy retention.

Author Contributions: Conceptualization, Y.Y. and Z.D.; methodology, Z.D.; validation, Z.D.; resources, Y.Y., H.C., Y.X. and J.Y.; writing—original draft, Z.D.; writing—review and editing, Z.D.; supervision, Y.X., H.C. and J.Y.; project administration, Y.Y., Y.X. and H.C. All authors have read and agreed to the published version of the manuscript.

Funding: This work was supported by the Special Project of the Ministry of Industry and Information Technology (Approval No. TC220H05V), the Henan province science and technology research project (Approval No. 242102220051), and the Key Scientific Research Projects of Universities in Henan Province (Approval No. 25CY007).

Data Availability Statement: The authors confirm that the data supporting the findings of this study are available within the article.

Conflicts of Interest: The authors declare no conflicts of interest.

Nomenclature

Symbol	Parameter
A	the contact area of roughness (m^2)
A_1	wear cross-section area (m^2)
B	wear cross-section width (m)
Δb	surface topography measuring instrument to measure the spacing (m)
D	circumference of the center circle of the wear trace (m)
E	effective Young's modulus, $\frac{1}{E} = \frac{1}{2}\left(\frac{1-v_1^2}{E_1} + \frac{1-v_2^2}{E_2}\right)$ (Pa)
E_1, E_2	rolling element and outer grove surface Young's modulus (Pa)
h	oil field rotary bit film thickness (m)
h_{min}	DOWSON minimum oil film thickness (m)
h_0	undeformed gap between two contact surfaces (m)
h_0'	uncorrected two-surface gap (m)
K	coefficient of wear
K_1	equivalent wear coefficient
L	sliding distance
p	contact pressure (hydrodynamic pressure and roughness contact pressure), (Pa)
P	non-dimensional pressure (dimensionless parameter, $P = p/p_h$)
p_l	hydrodynamic pressure (Pa)
p_h	maximum Hertz pressure (Pa)
p_c	roughness contact pressure (Pa)
R_x, R_y	effective radius in x-z and y-z plane (m)
R_{x1}, R_{x2}	radius of curvature of surfaces 1 and 2 in x-z plane (m)

R_{y1}, R_{y2}	radius of curvature of surfaces 1 and 2 in y-z plane (m)
S	slide–roll ratio $\left(\mathrm{S} = \frac{\lvert u_1+u_2 \rvert}{u_s}\right)$
t	wear time (s)
Δt	time step
u_s	entrainment speed $\left(u_s = \frac{(u_1+u_2)}{2}\right)$, (m/s)
u_1, u_2	linear velocity for surface 1 and 2 (m/s)
Δu	relative sliding velocity (m/s)
v	elastic deformation
v_1, v_2	Poisson's ratio for surfaces 1 and 2
W	normal load (N)
W_z	rolling element bears the load (N)
w_1, w_2	wear height of rough peak for surfaces 1 and 2 (μm)
x	x coordinate
y	y coordinate
x_0, x_e	the initial and end point coordinates in the x direction
y_0, y_e	the initial and end point coordinates in the y direction
ρ	density (g/m^3)
ρ_0	initial density of the lubricating oil (g/m^3)
η	viscosity (Pa·s)
η_0	initial viscosity of the lubricating oil (Pa·s)
δ_1, δ_2	roughness heights for surfaces 1 and 2 (μm)
Ω	solution region of Reynolds equation (m^2)
Ω_l	fluid lubrication region (m^2)
Ω_c	roughness contact area (m^2)
α	pressure–viscosity exponent (m^2·N^{-1})
λ	film thickness ratio
σ_0	root mean square of the composite roughness ($\sigma_0 = \sqrt{\sigma_1^2 + \sigma_2^2}$) (μm)
σ_1, σ_2	root mean square of roughness from surface 1 and 2 (μm)

References

1. Guo, F.; Li, X.; Lou, W.; Ma, Z.; Fu, Y. Several problems in the study of rolling bearing lubrication. *Bearing* **2024**, 1–20. [CrossRef]
2. Xu, F.; Ding, N.; Li, N.; Liu, L.; Hou, N.; Xu, N.; Guo, W.; Tian, L.; Xu, H.; Wu, C.-M.L. A review of bearing failure Modes, mechanisms and causes. *Eng. Fail. Anal.* **2023**, *152*, 107518. [CrossRef]
3. Vencl, A.; Gašić, V.; Stojanović, B. Fault tree analysis of most common rolling bearing tribological failures. *IOP Conf. Ser. Mater. Sci. Eng.* **2017**, *174*, 012048. [CrossRef]
4. Liu, H.; Chen, Y.; Guo, Y.; Shi, Y.; Chen, X. Precision Lifetime Analysis of High-Speed Machine Tool Bearings Based on Quasi-Static and Mixed Thermal Elastohydrodynamic Lubrication Models. *J. Tribology* **2025**, *45*, 1–24. [CrossRef]
5. Zhu, D.; Wang, Q.J. Effect of roughness orientation on the elastohydrodynamic lubrication film thickness. *J. Tribol.* **2013**, *135*, 031501. [CrossRef]
6. Masjedi, M.; Khonsari, M.M. An engineering approach for rapid evaluation of traction coefficient and wear in mixed EHL. *Tribol. Int.* **2015**, *92*, 184–190. [CrossRef]
7. Jiang, X.; Hua, D.Y.; Cheng, H.S.; Ai, X.; Lee, S.C. A mixed elastohydrodynamic lubrication model with asperity contact. *ASME J. Tribol.* **1999**, *121*, 481–491. [CrossRef]
8. Patir, N. An average flow model for determining effects of three-dimensional roughness on partial hydrodynamic lubrication. *Trans. ASME J. Lub. Tech.* **1979**, *101*, 220. [CrossRef]
9. Zhu, D.; Hu, Y.Z. The study of transition from elastohydrodynamic to mixed and boundary lubrication. *Adv. Front. Eng. Tribol. Proc. 1999 STLE/ASME HS Cheng Tribol. Surveill.* **1999**, 150–156.
10. Hu, Y.Z.; Zhu, D. A full numerical solution to the mixed lubrication in point contacts. *J. Tribol.* **2000**, *122*, 1–9. [CrossRef]
11. Zhu, D.; Martini, A.; Wang, W.; Hu, Y.; Lisowsky, B.; Wang, Q.J. Simulation of Sliding Wear in Mixed Lubrication. *J. Tribol.* **2007**, *129*, 544–552. [CrossRef]
12. Pei, X.; Pu, W.; Zhang, Y.; Huang, L. Surface topography and friction coefficient evolution during sliding wear in a mixed lubricated rolling-sliding contact. *Tribol. Int.* **2019**, *137*, 303–312. [CrossRef]

13. Zhao, J.; Li, Z.; Zhang, H.; Zhu, R. Study on sliding wear characteristics of non-gaussian rough surface in mixed lubrication. *Lubr. Sci.* **2022**, *34*, 27–139. [CrossRef]
14. Pu, W. Effect of surface topography associated with arbitrary velocity direction on the lubrication film thickness in elliptical contacts. *Ind. Lubr. Tribol.* **2018**, *70*, 444–452. [CrossRef]
15. Wang, D.; Yang, J.; Wei, P.; Pu, W. A mixed EHL model of grease lubrication considering surface roughness and the study of friction behavior. *Tribol. Int.* **2021**, *154*, 106710. [CrossRef]
16. Liu, H.; Chen, Y.; Wang, X.; Guo, Y.; Xue, W.; Li, D.; Chen, X.Q. Correlating numerical modelling with experimental studies to quantify the wear resistance of high-carbon chromium bearing steel in mixed lubrication. *Tribol. Int.* **2023**, *188*, 108819. [CrossRef]
17. Niu, R.; Luo, R.; Wang, Y.; Li, H.; Deng, S. Dynamic characteristics of angular contact ball bearings considering wear effects. *Journal of Vibration and Shock.* **2022**, *41*, 84–93. [CrossRef]
18. Niu, R.; Han, Z.; Wang, Y.; Li, H.; Deng, S. Wear life analysis of angular contact ball bearings under high temperature environment. *Aerodynamics* **2022**, *37*, 1780–1792. [CrossRef]
19. Chen, R.; Zhao, B.; Tu, L.; Xie, Z.; Lu, X.; Zou, D. Modelling and theoretical research on transient lubrication and wear coupling behavior of main bearing during start-up of low-speed diesel engine. *Proc. Inst. Mech. Eng. Part J J. Eng. Tribol.* **2024**, *239*, 13506501241294140. [CrossRef]
20. Chen, R.; Zhao, B.; Tu, L.; He, T.; Zhong, N.; Zou, D. Study on the coupling characteristics of thermo-elastohydrodynamic mixed lubrication and wear of main bearing of low-speed diesel engine. *Ship Mech.* **2024**, *28*, 1768–1779.
21. Colas, G.; Saulot, A.; Michel, Y.; Filleter, T.; Merstallinger, A. Experimental analysis of friction and wear of self-lubricating composites used for dry lubrication of ball bearing for space applications. *Lubricants* **2021**, *9*, 38. [CrossRef]
22. Shi, X.; Sun, W.; Lu, X.; Ma, X.; Zhu, D.; Zhao, B.; He, T. Three-dimensional mixed lubrication analysis of spur gears with machined roughness. *Tribol. Int.* **2019**, *140*, 105864. [CrossRef]
23. Shi, X.; Lu, X.; Feng, Y.; Qiu, Z. Tribo-dynamic analysis for aero ball bearing with 3D measured surface roughness. *Eng. Fail. Anal.* **2022**, *131*, 105848. [CrossRef]
24. Feng, Y.; Shi, X.J.; Lu, X.Q.; Sun, W.; Liu, K.P.; Fei, Y.F. Study on scuffing failure of gas turbine ball bearing based on 3D mixed lubrication and dynamics. *Proc. Inst. Mech. Eng. Part J J. Eng. Tribol.* **2024**, *238*, 897–911. [CrossRef]
25. Feng, Y.; Shi, X.J.; Lu, X.Q.; Sun, W.; Liu, K.P.; Fei, Y.F. Predictions of friction and wear in ball bearings based on a 3D point contact mixed EHL model. *Surf. Coat. Technol.* **2025**, *502*, 131939. [CrossRef]
26. Feng, Y.; Qiu, Z.; Shi, X.; Lu, X.; Sun, W.; Hua, D.; Sun, H. The Coupling Mechanism of Wear and Mixed Lubrication for Gas Turbine Ball Bearing Consider-ing Real Rough Surfaces. *J. Mech. Eng.* **2023**, *59*, 330–340.
27. Hamrock, B.J.; Dowson, D. Isothermal Elastohydrodynamic Lubrication of Point Contacts: Part IV—Starvation Results. *ASME. J. Lubr. Tech.* **1977**, *99*, 15–23. [CrossRef]
28. Zhao, J.; Wang, Z.; Li, Z.; Zhang, H.; Zhu, R. Fractal variation of three-dimensional surface topography during sliding wear under mixed elastohydrodynamic lubrication. *Surf. Topogr. Metrol. Prop.* **2021**, *9*, 045007. [CrossRef]
29. Guo, F.; Yang, P.; Qu, S. On the theory of thermal elastohydrodynamic lubrication at high slide-roll ratios—Circular glass-steel contact solution at opposite sliding. *J. Tribol.* **2001**, *123*, 816–821. [CrossRef]
30. Liu, Y.; Wang, Q.J.; Wang, W.; Hu, Y.; Zhu, D. Effects of Differential Scheme and Mesh Density on EHL Film Thickness in Point Contacts. *ASME. J. Tribol.* **2006**, *128*, 641–653. [CrossRef]
31. Meng, H.C.; Ludema, K.C. Wear models and predictive equations: Their form and content. *Wear* **1995**, *181*, 443–457. [CrossRef]
32. Chen, S.; Wang, Y.; Li, S.; Xin, H.; Li, H. Mathematical model of friction coefficient and wear loss of MoS2 film. *Surf. Technol.* **2022**, *51*, 51–56+75. [CrossRef]
33. Dai, X.; Lai, Y. A method of wear prediction-IBM method. *Mech. Dev.* **1985**, 15–23+8.

Disclaimer/Publisher's Note: The statements, opinions and data contained in all publications are solely those of the individual author(s) and contributor(s) and not of MDPI and/or the editor(s). MDPI and/or the editor(s) disclaim responsibility for any injury to people or property resulting from any ideas, methods, instructions or products referred to in the content.